

Improved electrochemical properties of YF₃-coated Li_{1.2}Mn_{0.54}Ni_{0.13}Co_{0.13}O₂ as cathode for Li-ion batteries

Bailong Liu^{1,2} · Zhaohui Zhang^{1,2} · Jiangkai Wan¹ · Shifeng Liu^{1,2}

Received: 5 November 2016 / Revised: 10 December 2016 / Accepted: 18 December 2016 / Published online: 5 January 2017
© Springer-Verlag Berlin Heidelberg 2017

Abstract Yttrium fluoride YF₃ layer with different coating contents is successfully covered on the surface of Li_{1.2}Mn_{0.54}Ni_{0.13}Co_{0.13}O₂ via a common wet chemical approach. The XRD, SEM, TEM, and charge-discharge tests are applied to investigate the influence of YF₃ layer on the microstructural, morphology, and electrochemical properties of Li_{1.2}Mn_{0.54}Ni_{0.13}Co_{0.13}O₂. And the electrochemical test results demonstrate that the YF₃-coated LMNCO samples exhibit the improved electrochemical properties. The 2wt.%YF₃-coated LMNCO delivers a discharge capacity of 116.6 mAh g⁻¹ at 5 C rate, much larger than that (95.6 mAh g⁻¹) of the pristine one. Besides, the electrochemical impedance spectroscopy (EIS) and cyclic voltammetric results indicate that the YF₃ coating layer can promote the optimization formation of SEI film and reversibility of the electrochemical redox.

Keywords Li_{1.2}Mn_{0.54}Ni_{0.13}Co_{0.13}O₂ · YF₃-coated · Electrochemical properties · Lithium-ion battery

Introduction

Nowadays, the Li-ion batteries have been widely used for Electronic Consumer Market, Electric Vehicle Sector, and so

on [1, 2]. However, owing to the low mass energy density of cathode materials, such as LiCoO₂, LiFePO₄, and LiMn_{1/3}Ni_{1/3}Co_{1/3}O₂, the Li-ion batteries cannot be applied in the high power output equipment [3–5]. As a probable alternative to the traditional cathode materials, layered lithium-rich materials xLi₂MnO₃·(1-x)LiMO₂ (M = Ni, Co, Mn, etc) can deliver a high specific discharge capacity (up to 250 mAh g⁻¹) and become appealing for practical application in the electric vehicles (EVs) and hybrid electric vehicles (HEVs) [6, 7]. However, some drawbacks, such as the large initial irreversible capacity loss and poor cycling performance at high current density, have limited the applications of the materials [8, 9]. To circumvent the abovementioned intrinsic limitations, a most conventional and efficient method is to cover the surface of pristine particle with metal oxides [10, 11], phosphates [12, 13], fluorides [14], etc. These modifying layers can reduce the initial irreversible capacity loss and improve the cycling performance of the layered lithium-rich materials through inhibiting the side reaction between the cathode and electrolyte during the charge-discharge process.

It has been proven that HF species will be formed by the hydrolysis of electrolyte with a trace amount of water [15]. And metal fluorides have demonstrated chemical stable under the environment of HF acid etching [16]. Therefore, metal fluoride is one of the most promising surface coating candidates. Besides, among the doping modification elements, rare earth elements have been tested to be a superior choice for doping into layered lithium-rich materials due to the high stability under harsh environmental conditions of attacks by moisture or chemical reactions [17]. For example, when Y³⁺ was doped into Li[Li_{0.20}Mn_{0.534}Ni_{0.133}Co_{0.133}]O₂ via coprecipitation method, Li[Li_{0.20}Mn_{0.534}Ni_{0.133}Co_{0.133-x}Y_x]O₂ (x = 0.00665) delivered a specific discharge capacity of 225.2 mAh g⁻¹ after 80 cycles with a current rate of 0.1 C between 2.0 and 4.6 V vs Li/Li⁺, while the unsubstituted

✉ Zhaohui Zhang
xauatme@foxmail.com

¹ School of Metallurgical Engineering, Xi'an University of Architecture and Technology, Xi'an 710055, People's Republic of China

² Shaanxi Province Metallurgical Engineering and Technology Research Centre, Xi'an University of Architecture and Technology, Xi'an 710055, People's Republic of China

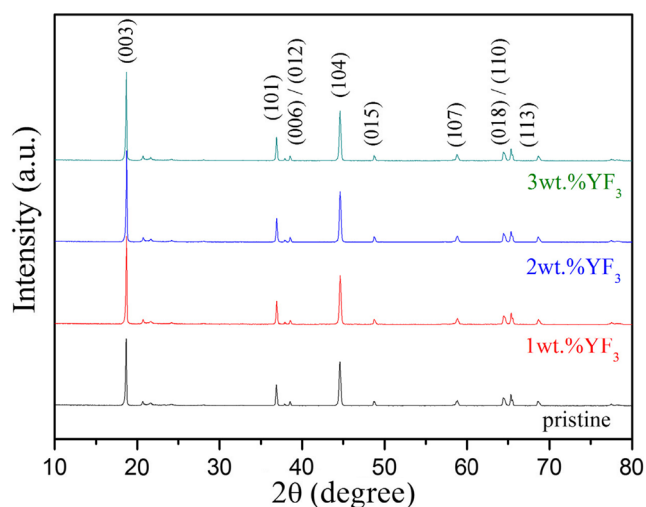


Fig. 1 XRD patterns of $\text{Li}_{1.2}\text{Mn}_{0.54}\text{Ni}_{0.13}\text{Co}_{0.13}\text{O}_2$ samples before and after YF_3 surface coating

material $\text{Li}[\text{Li}_{0.20}\text{Mn}_{0.534}\text{Ni}_{0.133}\text{Co}_{0.133}]\text{O}_2$ only retained 163.6 mAh g^{-1} [18]. Based on the above discussion, YF_3 will be an attractive modification material to cover on the surface of the layered lithium-rich cathode particles.

In the work, the pristine $\text{Li}_{1.2}\text{Mn}_{0.54}\text{Ni}_{0.13}\text{Co}_{0.13}\text{O}_2$ was synthesized via using carbonate co-precipitation method. And then a common wet chemical approach was employed to cover the $\text{Li}_{1.2}\text{Mn}_{0.54}\text{Ni}_{0.13}\text{Co}_{0.13}\text{O}_2$ nanoparticles with the thin Ytterbium fluoride (YF_3) layer. The surface morphology, microstructural, and electrochemical performance were investigated to evaluate the influence of different YF_3 coating amount on the surface of $\text{Li}_{1.2}\text{Mn}_{0.54}\text{Ni}_{0.13}\text{Co}_{0.13}\text{O}_2$ cathode.

Experimental

Material preparation

The precursor $[\text{Mn}_{0.54}\text{Ni}_{0.13}\text{Co}_{0.13}](\text{CO}_3)_{0.8}$ powders was prepared via using carbonate co-precipitation method [13], that is, the Na_2CO_3 solution was used to precipitate the NiSO_4 , CoSO_4 , and MnSO_4 solutions uniformly. And then a homogeneous mixture containing the stoichiometric amount of $[\text{Mn}_{0.54}\text{Ni}_{0.13}\text{Co}_{0.13}](\text{CO}_3)_{0.8}$ and an excess 3 wt.% amount

of $\text{LiOH}\cdot\text{H}_2\text{O}$ was pre-heated at 500°C for 5 h and sintered at 950°C for 12 h to obtain the target product $\text{Li}_{1.2}\text{Mn}_{0.54}\text{Ni}_{0.13}\text{Co}_{0.13}\text{O}_2$ (LMNCO).

The YF_3 -coated $\text{Li}_{1.2}\text{Mn}_{0.54}\text{Ni}_{0.13}\text{Co}_{0.13}\text{O}_2$ cathode was prepared via using wet chemical approach as follows: (1) the pristine $\text{Li}_{1.2}\text{Mn}_{0.54}\text{Ni}_{0.13}\text{Co}_{0.13}\text{O}_2$ powders were homogeneously dispersed into the $\text{Y}(\text{NO}_3)_3$ solution with continuous stirring, followed by the slow addition of stoichiometric amount of NH_4F solution; (2) the obtained suspension solution was dried in vacuum at 100°C , followed by a slow evaporation of solvent; (3) the prepared powders were calcined at 400°C for 4 h in a flowing N_2 to get the YF_3 -coated $\text{Li}_{1.2}\text{Mn}_{0.54}\text{Ni}_{0.13}\text{Co}_{0.13}\text{O}_2$ powder. While the contents of YF_3 in the pristine cathode varied from 1, 2, and 3 wt.%, that is 1 wt.% YF_3 -coated $\text{Li}_{1.2}\text{Mn}_{0.54}\text{Ni}_{0.13}\text{Co}_{0.13}\text{O}_2$ (1 wt.% YF_3 -LMNCO), 2 wt.% YF_3 -coated $\text{Li}_{1.2}\text{Mn}_{0.54}\text{Ni}_{0.13}\text{Co}_{0.13}\text{O}_2$ (2 wt.% YF_3 -LMNCO), and 3 wt.% YF_3 -coated $\text{Li}_{1.2}\text{Mn}_{0.54}\text{Ni}_{0.13}\text{Co}_{0.13}\text{O}_2$ (3 wt.% YF_3 -LMNCO).

Material characterization

The micro-structures of the pristine and YF_3 -coated $\text{Li}_{1.2}\text{Mn}_{0.54}\text{Ni}_{0.13}\text{Co}_{0.13}\text{O}_2$ were measured by X-ray diffraction (XRD) using Bruker D8 Advance X-ray diffractometer with $\text{Cu } K_\alpha$ radiation in the 2θ range of $10^\circ\sim 80^\circ$. The morphologies of synthesized materials were characterized by using scanning electron microscopy (FE-SEM, JSM-7001F, JEOL) coupled with an energy dispersive spectrum X-ray detector (EDS) to analyze the element composition. More distinct morphologies were compared by transmission electron microscope (TEM, JEOL JEM 2010).

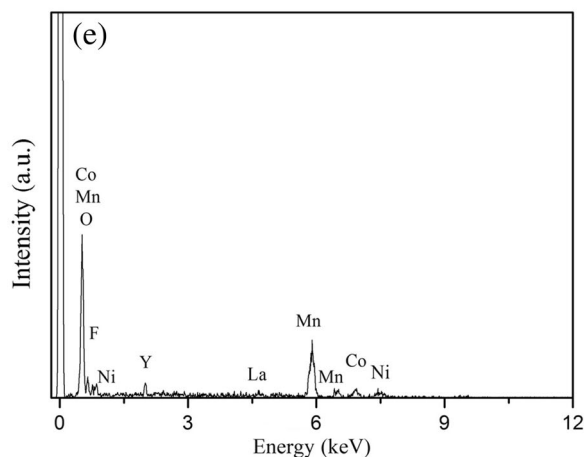
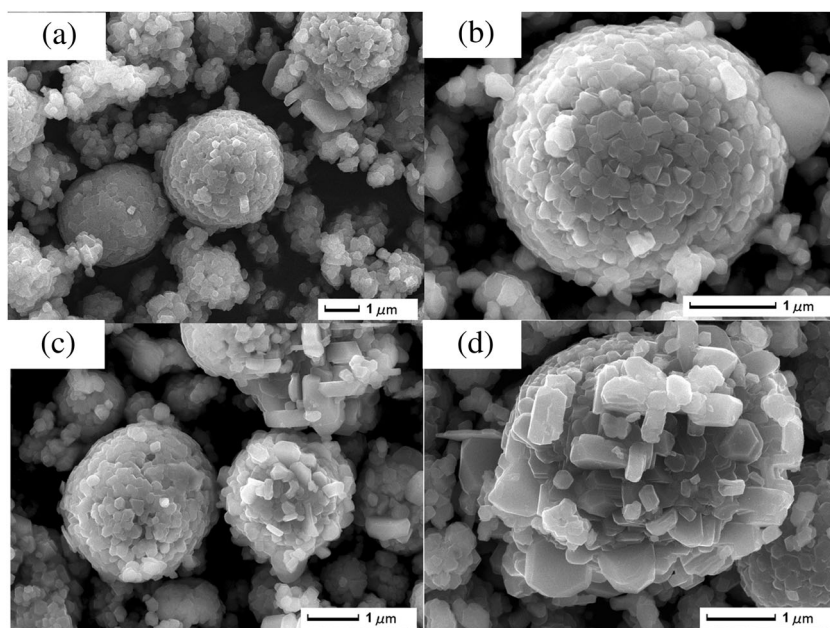
Electrochemical characterization

Electrochemical properties of the pristine and YF_3 -coated $\text{Li}_{1.2}\text{Mn}_{0.54}\text{Ni}_{0.13}\text{Co}_{0.13}\text{O}_2$ samples were characterized by using CR2025 coin cell. Cell was consisted of as-prepared cathode, metallic Li foil anode, and Celgard 2320 membrane. The cathode was prepared as follows: a mixture containing 75 wt.% the pristine and YF_3 -coated $\text{Li}_{1.2}\text{Mn}_{0.54}\text{Ni}_{0.13}\text{Co}_{0.13}\text{O}_2$ materials, 15 wt.% Super P conductive additive and 10 wt.% polyvinylidene fluoride was stirred in 1-methyl-2-pyrrolidone solvent to form the cathode slurry. Then, the slurry was cast on

Table 1 Values of $I_{(003)}/I_{(104)}$ and lattice parameter of $\text{Li}_{1.2}\text{Mn}_{0.54}\text{Ni}_{0.13}\text{Co}_{0.13}\text{O}_2$ samples before and after YF_3 surface coating

Sample	a (Å)	c (Å)	c/a	$R = I_{(003)}/I_{(104)}$
pristine LMNCO	2.853	14.220	4.984	1.520
1 wt.% YF_3 -LMNCO	2.852	14.228	4.989	1.780
2 wt.% YF_3 -LMNCO	2.853	14.236	4.990	1.790
3 wt.% YF_3 -LMNCO	2.858	14.274	4.994	1.750

Fig. 2 SEM images of the $\text{Li}_{1.2}\text{Mn}_{0.54}\text{Ni}_{0.13}\text{Co}_{0.13}\text{O}_2$ before (a) and after the surface coating with 1 wt.% YF_3 (b), 2 wt.% YF_3 (c), and 3 wt.% YF_3 (d). EDS spectra of 2 wt.% YF_3 -coated $\text{Li}_{1.2}\text{Mn}_{0.54}\text{Ni}_{0.13}\text{Co}_{0.13}\text{O}_2$ (e)



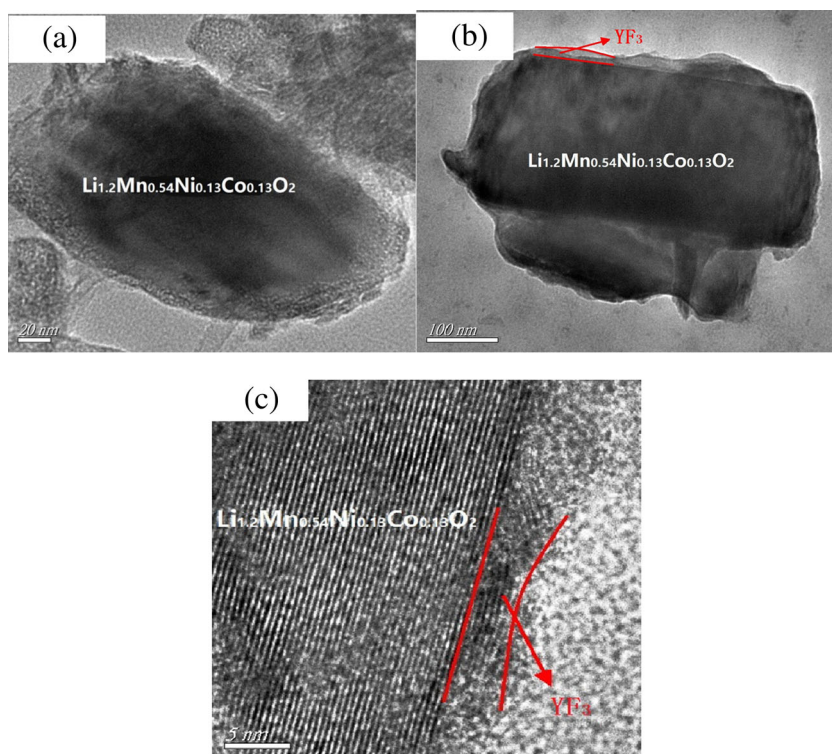
Al foil, followed by being cut into circular disk with $d = 12$ mm, that is the final cathode. The CR2025 cells were packaged in glove box filled with argon, while the LiPF_6 (1 M) in EC/DMC (a mass ratio of 1:1) was served as electrolyte. The Electrochemical properties were evaluated on LAND CT-2001A instrument at 25 °C. The CHI660D workstation was used to measure the electrochemical impedance spectroscopy (a frequency range from 0.01 Hz to 100 kHz and perturbation amplitude of 5 mV) and the cyclic voltammogram (a voltage range from 2.0 to 4.8 V with a scanning rate of 0.1 mV s^{-1}).

Results and discussion

The XRD patterns of $\text{Li}_{1.2}\text{Mn}_{0.54}\text{Ni}_{0.13}\text{Co}_{0.13}\text{O}_2$ samples before and after the YF_3 surface coating are shown in Fig. 1. All the diffraction peaks of synthesized samples correspond to α -

NaFeO_2 hexagonal structure with a space group of R-3 m, except for the weak peaks between 20° and 25° , identified as LiMn_6 cation arrangement in the transition metal layer with the monoclinic unit cell C2/m [18, 19]. The four samples all show that the adjacent peaks of (006)/(102) and (018)/(110) separate clearly, indicating that the well-layered structure with a good crystallinity is formed [20]. Besides, all the diffraction peaks of after YF_3 surface coating samples are similar to the pristine one and no peaks corresponding to the YF_3 are discovered owing to the poor crystallinity or low coating amount of YF_3 . Table 1 shows the value of $I_{(003)}/I_{(104)}$ and lattice parameter of $\text{Li}_{1.2}\text{Mn}_{0.54}\text{Ni}_{0.13}\text{Co}_{0.13}\text{O}_2$ samples before and after YF_3 surface coating. The integrated ratio of $I_{(003)}/I_{(104)}$ (R) peaks in XRD patterns is regarded as a measurement of the cation-mixing, especially a value of $R > 1.2$ is an indicator of desirable cation-mixing between Li^+ and Ni^{2+} [21]. With the YF_3 surface coating content increasing, the intensity ratios of $I_{(003)}/I_{(104)}$ are 1.520, 1.780, 1.790, and 1.750, respectively,

Fig. 3 TEM image of pristine $\text{Li}_{1.2}\text{Mn}_{0.54}\text{Ni}_{0.13}\text{Co}_{0.13}\text{O}_2$ (a), 2 wt.% YF_3 -coated $\text{Li}_{1.2}\text{Mn}_{0.54}\text{Ni}_{0.13}\text{Co}_{0.13}\text{O}_2$ (b), HRTEM image of 2wt.% YF_3 -coated $\text{Li}_{1.2}\text{Mn}_{0.54}\text{Ni}_{0.13}\text{Co}_{0.13}\text{O}_2$ (c)



implying that the low cation mixing is formed in the synthesized samples. The higher value of $I_{(003)}/I_{(104)}$ ratio for the surface coating samples maybe related to the partial substitution of Y^{3+} from YF_3 into the layered lattice of cathode [22]. And the Y^{3+} can partially substitute Co^{3+} in transition metal layer and also cause the increase of parameter c [23, 24]. When the c lattice parameter increases, the diffraction intensity of (003) peak can also enhance, resulting in the larger

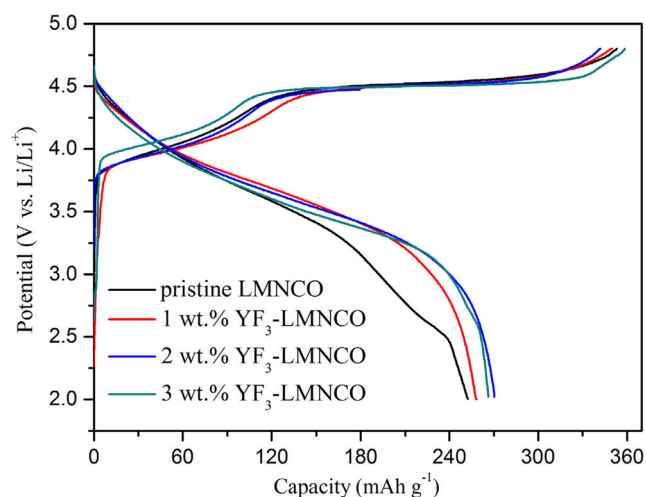


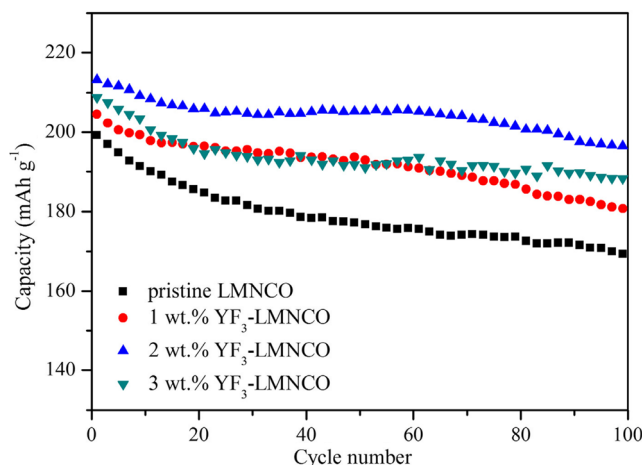
Fig. 4 Initial charge and discharge profiles of $\text{Li}_{1.2}\text{Mn}_{0.54}\text{Ni}_{0.13}\text{Co}_{0.13}\text{O}_2$ samples before and after YF_3 surface coating from 2.0 to 4.8 V at 0.1 C rate

value of $I_{(003)}/I_{(104)}$ ratio. Meanwhile, the value of c/a is related to the stability of layered structure [25]. The four samples all deliver a high value of c/a (larger than 4.90), indicating that they have formed stable layer structure.

Figure 2 shows the SEM images of the $\text{Li}_{1.2}\text{Mn}_{0.54}\text{Ni}_{0.13}\text{Co}_{0.13}\text{O}_2$ before and after the YF_3 surface coating. All samples present similar spherical secondary particles with particle size from 3 to 5 μm , which are composed of numerous primary particles. With the YF_3 coating content increasing, the surface of synthesized samples appears more rough due to some micro-size particles adhered to the bulk of LMNCO, which perhaps correspond to the YF_3 coating material. Figure 2e shows the EDS spectra of 2 wt.% YF_3 -coated $\text{Li}_{1.2}\text{Mn}_{0.54}\text{Ni}_{0.13}\text{Co}_{0.13}\text{O}_2$ sample, and the detection of F and Y element has demonstrated the existence of YF_3 surface coating layer. Figure 3 shows the TEM image of pristine $\text{Li}_{1.2}\text{Mn}_{0.54}\text{Ni}_{0.13}\text{Co}_{0.13}\text{O}_2$ and 2 wt.% YF_3 -coated $\text{Li}_{1.2}\text{Mn}_{0.54}\text{Ni}_{0.13}\text{Co}_{0.13}\text{O}_2$ sample. In comparison with the pristine LMNCO, the surface of YF_3 -coated LMNCO particles has been covered by the YF_3 layer with a thickness from 10 to 30 nm, while the pristine particle shows a smooth edge lines without other surface adhesive materials. Figure 3c shows the HR-TEM image of 2 wt.% YF_3 -coated $\text{Li}_{1.2}\text{Mn}_{0.54}\text{Ni}_{0.13}\text{Co}_{0.13}\text{O}_2$ particles. The distinct lattice fringes can be observed in the $\text{Li}_{1.2}\text{Mn}_{0.54}\text{Ni}_{0.13}\text{Co}_{0.13}\text{O}_2$ bulk. In addition, it can be calculated that the interplanar distance of the lattice fringes is 0.47 nm, which is indexed to the (003)

Table 2 Initial charge-discharge data of $\text{Li}_{1.2}\text{Mn}_{0.54}\text{Ni}_{0.13}\text{Co}_{0.13}\text{O}_2$ samples before and after YF_3 surface coating at 0.1 C rate in the voltage range of 2.0–4.8 V

Sample	Specific charge capacity (mAh g^{-1})	Specific discharge capacity (mAh g^{-1})	Irreversible capacity loss (mAh g^{-1})	Coulombic efficiency (%)
pristine LMNCO	353.0	254.7	98.3	72.2
1 wt.% YF_3 -LMNCO	350.1	260.3	89.8	74.4
2 wt.% YF_3 -LMNCO	344.5	270.3	74.2	78.5
3 wt.% YF_3 -LMNCO	355.5	267.3	88.2	75.2

**Fig. 5** Cycling performance of $\text{Li}_{1.2}\text{Mn}_{0.54}\text{Ni}_{0.13}\text{Co}_{0.13}\text{O}_2$ samples before and after YF_3 surface coating at 0.5 C rate in the voltage range of 2.0–4.6 V

crystal plane of the hexagonal layered phase, implying the intact hexagonal ordering structure after surface modification for 2wt.% YF_3 -coated $\text{Li}_{1.2}\text{Mn}_{0.54}\text{Ni}_{0.13}\text{Co}_{0.13}\text{O}_2$. And no lattice fringes corresponding to YF_3 can be detected on the surface region, indicating that the YF_3 layer shows an amorphous phase on the sample surface. Based on the above discussion, the pristine LMNCO particles have indeed covered by a thin YF_3 layer.

The initial charge and discharge profiles of $\text{Li}_{1.2}\text{Mn}_{0.54}\text{Ni}_{0.13}\text{Co}_{0.13}\text{O}_2$ samples before and after YF_3 surface coating from 2.0 to 4.8 V at 0.1 C rate ($1\text{ C} = 250\text{ mA g}^{-1}$) are shown in Fig. 4. Two typical steps can be observed for the synthesized samples during the initial charge process. The charge voltage range of first step is from 2.0 to 4.5 V, corresponding to the Li^+ -extraction from the structure of space

group R-3m, along with the oxidation of Ni^{2+} to Ni^{4+} and Co^{3+} to Co^{4+} [26]. The charge voltage platform of second step is at 4.55 V, meaning the activation of the Li_2MnO_3 phase. The lithium-ion extract from the Li_2MnO_3 component irreversibly, resulting in a large irreversible capacity loss during the initial cycle [27]. Table 2 demonstrates the initial charge-discharge data of $\text{Li}_{1.2}\text{Mn}_{0.54}\text{Ni}_{0.13}\text{Co}_{0.13}\text{O}_2$ samples before and after YF_3 surface coating. The initial discharge capacities, respectively, are 260.3, 270.3 and 267.3 mAh g^{-1} for YF_3 -coated LMNCO electrodes with 1, 2, and 3 wt.% coating contents, larger than that (254.7 mAh g^{-1}) of the pristine LMNCO. Besides, the YF_3 coating layer also decreases the initial irreversible capacity loss of cathode materials. And when the YF_3 coating amount increases, the four samples severally exhibit the initial coulombic efficiency of about 72.2, 74.4, 78.5, and 75.2%. The main reason for the improvement maybe that the substitution of F^- for O^{2-} from YF_3 coating layer changes the electronic environment and prohibits the mobility or release of oxygen ions from Li_2MnO_3 component [28].

Figure 5 shows the cycling performance of $\text{Li}_{1.2}\text{Mn}_{0.54}\text{Ni}_{0.13}\text{Co}_{0.13}\text{O}_2$ samples before and after YF_3 surface coating at 0.5 C rate in the voltage range of 2.0–4.6 V. Compared with the pristine LMNCO, the samples after YF_3 surface coating obviously show a better cycling performance. Among the four samples, the 2wt.% YF_3 -coated LMNCO demonstrates the greatest cycling stability. Table 3 shows the capacity retention and discharge capacity of $\text{Li}_{1.2}\text{Mn}_{0.54}\text{Ni}_{0.13}\text{Co}_{0.13}\text{O}_2$ samples before and after YF_3 surface coating. When the YF_3 coating amount increases, the discharge capacities of $\text{Li}_{1.2}\text{Mn}_{0.54}\text{Ni}_{0.13}\text{Co}_{0.13}\text{O}_2$ samples before and after YF_3 surface coating are 199.3, 204.5, 213.1, and 208.8 mAh g^{-1} at the initial cycle, respectively. After

Table 3 Capacity retention and discharge capacity of $\text{Li}_{1.2}\text{Mn}_{0.54}\text{Ni}_{0.13}\text{Co}_{0.13}\text{O}_2$ samples before and after YF_3 surface coating at 0.5 C rate in the voltage range of 2.0–4.6 V

Sample	Initial discharge specific capacity (mAh g^{-1})	100th specific discharge capacity (mAh g^{-1})	100 cycles capacity retention (%)
pristine LMNCO	199.3	169.1	84.8
1 wt.% YF_3 -LMNCO	204.5	180.3	88.2
2 wt.% YF_3 -LMNCO	213.1	196.4	92.2
3 wt.% YF_3 -LMNCO	208.8	188.3	90.2

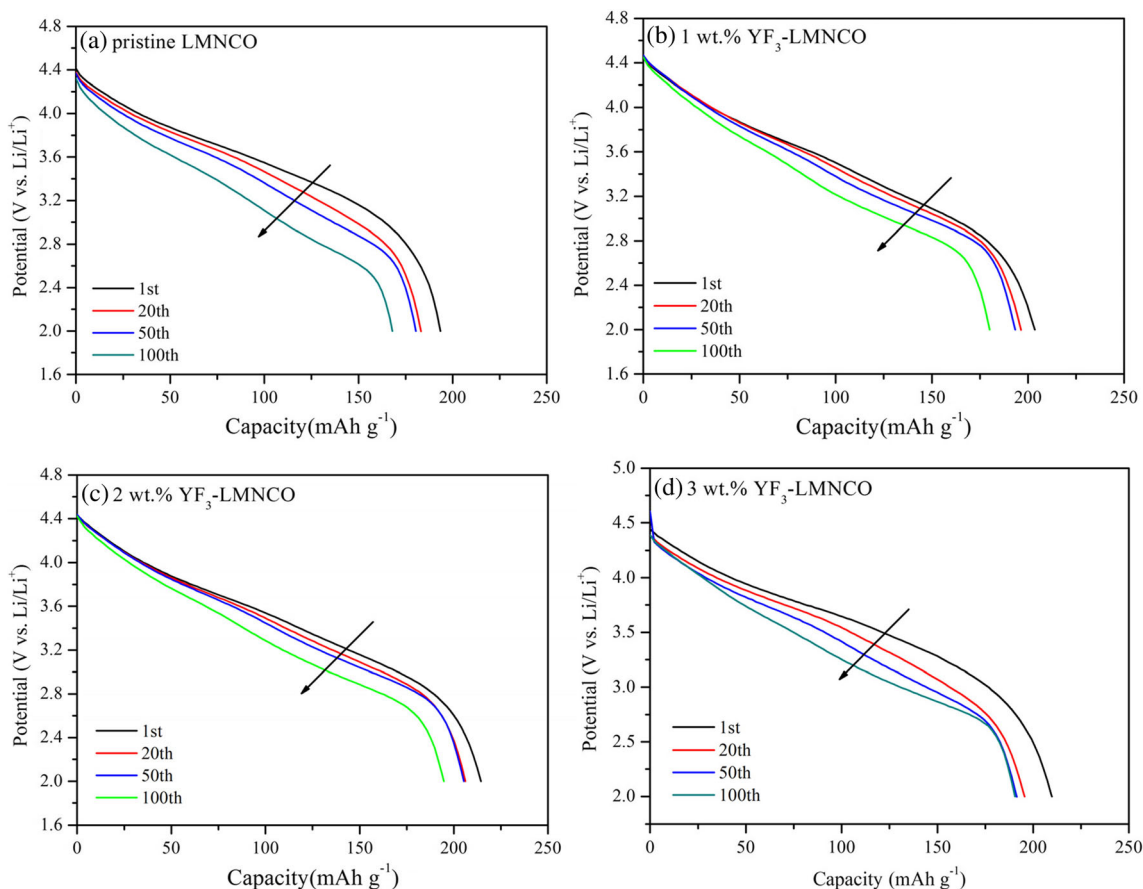


Fig. 6 Discharge profiles of $\text{Li}_{1.2}\text{Mn}_{0.54}\text{Ni}_{0.13}\text{Co}_{0.13}\text{O}_2$ samples before and after YF_3 surface coating in the 1st, 20th, 50th, and 100th cycles at 0.5 C rate

100 cycles, the discharge capacities of the pristine LMNCO as well as 1, 2, and 3 wt.% YF_3 -LMNCO are 169.1, 180.3, 196.4, and 188.3 mAh g^{-1} , respectively, corresponding that the capacity retentions firstly increase from 84.8% to 88.2% and 92.2%, and then decrease to 90.2%. It indicates that the capacity retentions of YF_3 -

coated LMNCO samples are much higher than those of the pristine one. Besides, Fig. 6 shows the discharge profiles of $\text{Li}_{1.2}\text{Mn}_{0.54}\text{Ni}_{0.13}\text{Co}_{0.13}\text{O}_2$ samples before and after YF_3 surface coating in the 1st, 20th, 50th, and 100th cycles at 0.5 C rate. With cycle going on, it can be observed that the discharge profiles shift to lower voltage plateaus for all electrodes (as indicated by the arrow), implying the increase of polarization with cycles. It can be calculated that the difference values of discharge mid-point voltage (ΔV) between 1st and 100th cycle are 0.24, 0.18, 0.16, and 0.19 V, respectively. The YF_3 -coated LMNCO samples deliver the smaller voltage decay than that of pristine one during cycling. The outstanding cycling performance and the smaller voltage decay for YF_3 -coated LMNCO samples have testified that YF_3 thin film could effectively restrict the side reaction between cathode materials and electrolyte, followed by protecting cathode materials from erosion by the electrolyte by-products during cycling. However, when the YF_3 coating content exceeds 2 wt.%, the cycling performance of YF_3 -coated LMNCO sample will worsen due to the poor electrical conductivity of the thick surface YF_3 layer [29].

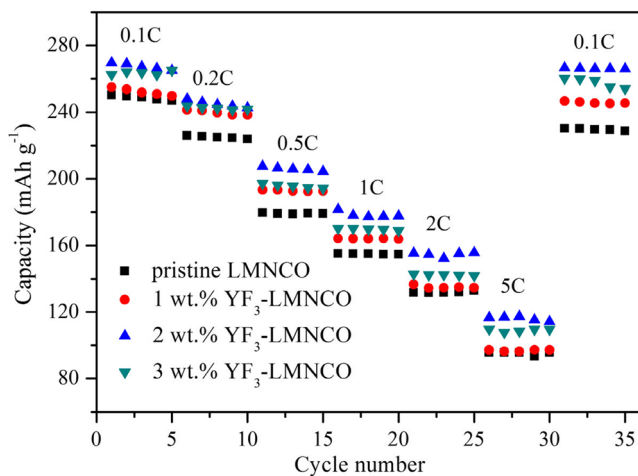


Fig. 7 Rate capability of $\text{Li}_{1.2}\text{Mn}_{0.54}\text{Ni}_{0.13}\text{Co}_{0.13}\text{O}_2$ samples before and after YF_3 surface coating at rates of 0.1, 0.2, 0.5, 1, 2, and 5 C in sequence for each 5 cycles

Figure 7 shows the rate capability of $\text{Li}_{1.2}\text{Mn}_{0.54}\text{Ni}_{0.13}\text{Co}_{0.13}\text{O}_2$ samples before and after YF_3

Table 4 Discharge capacity of $\text{Li}_{1.2}\text{Mn}_{0.54}\text{Ni}_{0.13}\text{Co}_{0.13}\text{O}_2$ samples before and after YF_3 surface coating at various current densities in the voltage range of 2.0–4.6 V

sample	0.1 C rate (mAh g ⁻¹)	0.2 C rate (mAh g ⁻¹)	0.5 C rate (mAh g ⁻¹)	1 C rate (mAh g ⁻¹)	2 C rate (mAh g ⁻¹)	5 C rate (mAh g ⁻¹)	follow-up 0.1 C rate (mAh g ⁻¹)
pristine LMNCO	250.3	225.9	179.6	155.1	131.8	95.6	230.3
1wt.% YF_3 -LMNCO	255.0	241.4	193.3	164	136.6	97.1	246.7
2 wt.% YF_3 -LMNCO	269.5	247.9	207.5	181.6	155.4	116.6	266.5
3 wt.% YF_3 -LMNCO	262.5	243.7	197.1	170.0	142.7	109.7	260.2

surface coating at rates of 0.1, 0.2, 0.5, 1, 2, and 5 C in sequence for each 5 cycles. It can be observed that the YF_3 -coated samples deliver a better rate capability than that of the pristine one. Besides, the applied current density increases; the superiority gap of rate capability becomes larger. Table 4 presents the discharge capacity of $\text{Li}_{1.2}\text{Mn}_{0.54}\text{Ni}_{0.13}\text{Co}_{0.13}\text{O}_2$ samples before and after YF_3 surface coating at various

current densities. Among the four samples, the 2wt.% YF_3 -coated LMNCO demonstrates a prime rate capability. When the current rate increases to 5 C, the 2wt.% YF_3 -coated LMNCO can deliver 116.6 mAh g⁻¹, much larger than that (95.6 mAh g⁻¹) of the pristine one. The prioritized rate capability can be ascribed that the existence of YF_3 coating layer has restrained the thickening of SEI film and accelerated the

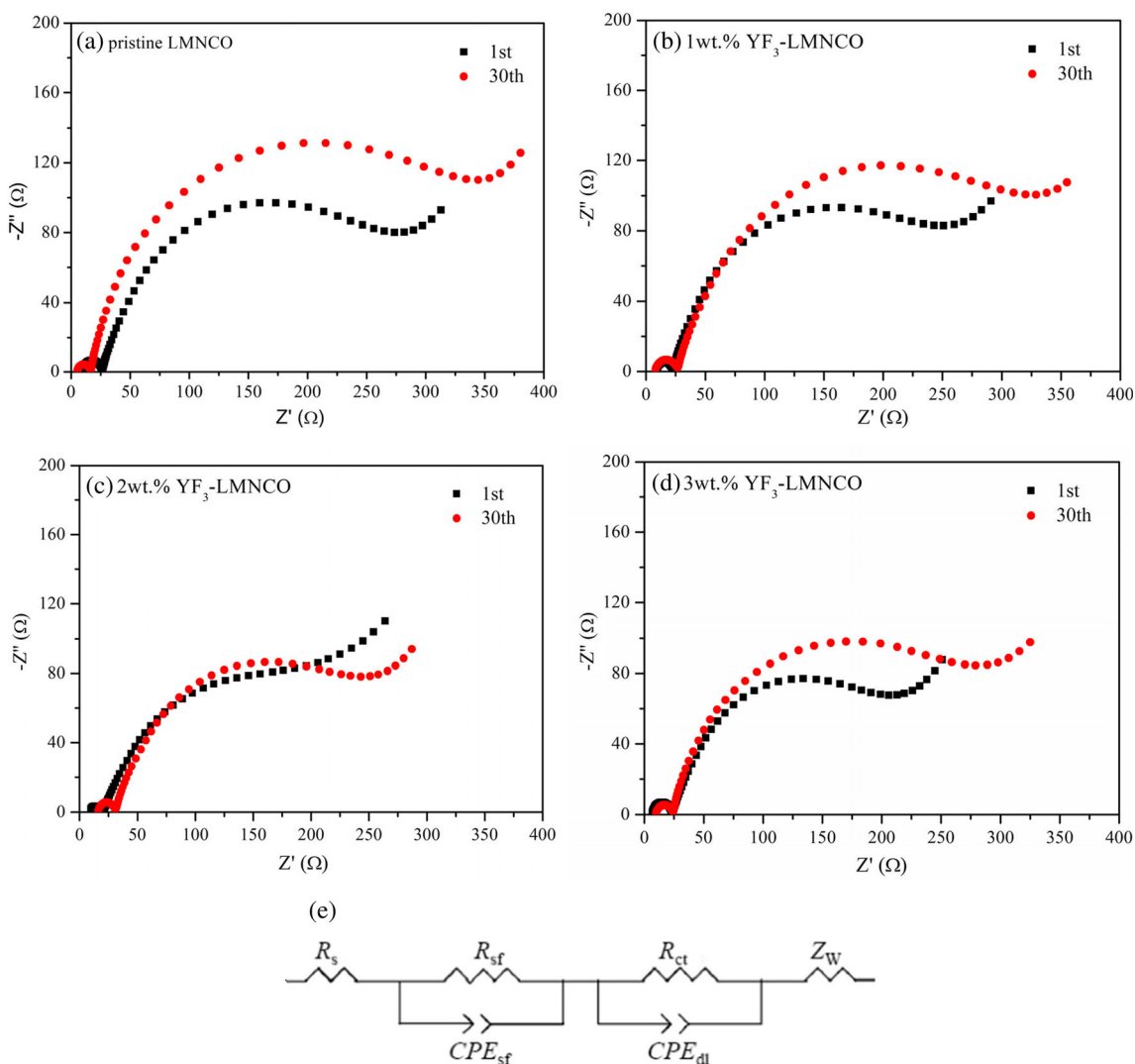


Fig. 8 Nyquist plots of $\text{Li}_{1.2}\text{Mn}_{0.54}\text{Ni}_{0.13}\text{Co}_{0.13}\text{O}_2$ samples before and after YF_3 surface coating at a charge state of 4.6 V in different cycles and the equivalent circuit (e)

Table 5 Values of R_s , R_f , and R_{ct} for $\text{Li}_{1.2}\text{Mn}_{0.54}\text{Ni}_{0.13}\text{Co}_{0.13}\text{O}_2$ samples before and after YF_3 surface coating at 4.6 V after different cycles

Sample	Cycle number	R_s (Ω)	R_{sf} (Ω)	R_{ct} (Ω)	ΔR_{sf} (Ω)
pristine LMNCO	1th	10.2	210.0	16.1	85.3
	30 th	11.3	295.3	16.5	
1 wt.% YF_3 -LMNCO	1th	8.3	182.2	13.1	66.3
	30 th	8.5	248.5	14.5	
2 wt.% YF_3 -LMNCO	1th	7.3	145.1	12.3	41.2
	30 th	8.4	186.3	14.5	
3 wt.% YF_3 -LMNCO	1th	8.1	158.2	14.2	61.2
	30 th	8.8	220.4	15.5	

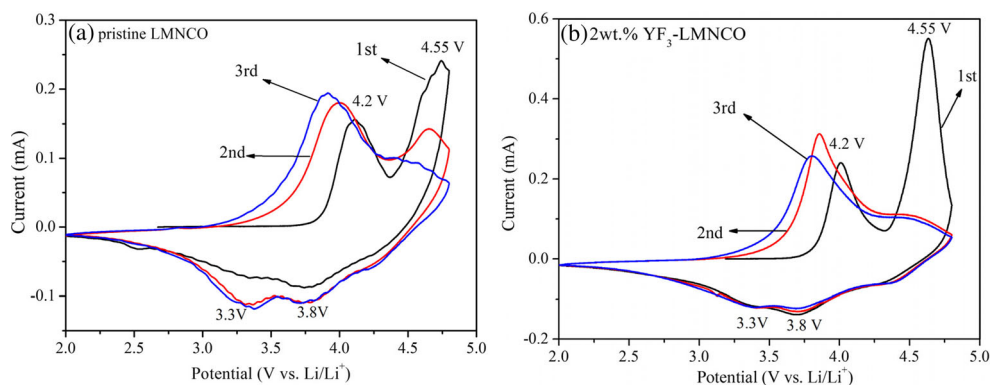
rate of Li^+ diffusion during cycling process [30]. Meanwhile, when cycled back at 0.1 C rate, a discharge capacity of 266.5 mAh g^{-1} is obtained for the 2wt.% YF_3 -coated LMNCO, corresponding to a capacity recovery of 98.9%, while the pristine LMNCO only delivers a capacity recovery of 92.0%. This result implies that the YF_3 thin film can promote the reversibility of Li^+ intercalation and deintercalation in SEI film [31].

It is generally known that the electrochemical properties of cathode are closely related to the electrochemical impedance. Therefore, the electrochemical impedance spectroscopy (EIS) for $\text{Li}_{1.2}\text{Mn}_{0.54}\text{Ni}_{0.13}\text{Co}_{0.13}\text{O}_2$ samples before and after YF_3 surface coating is measured, as seen in Fig. 8. And the Fig. 8e provides the corresponding equivalent circuit to calculate and analyze a quantitative result. All the Nyquist plots contain three parts as follows: a semicircle in the high frequency, a semicircle in the high to medium frequency, and a quasi-straight line in the low frequency, which respectively represent the impedance of Li^+ migration at the electrode/electrolyte interface (R_{sf} and CPE_{sf}), the impedance of charge transfer (R_{ct} and CPE_{dl}), and the impedance of Li-ion migration in the cathode (W), while R_s refers to the ohmic resistance of the cell [11]. According to corresponding equivalent circuit, the values of R_s , R_{sf} , and R_{ct} can be acquired by fitting ZSimpWin software, as is shown in Table 5. The side reaction between the cathode and electrolyte can generate some by-product, which will deposit at the electrode/electrolyte

interface to form the solid electrolyte interface (SEI) film. The SEI film will become thick during the cycling, corresponding to the enhancement of R_{sf} value [32]. With the cycles going, it can be seen that the value of ΔR_{sf} for the pristine LMNCO is larger than that of the YF_3 -coated LMNCO samples. The pristine LMNCO delivers an increasing value of R_{sf} from 210.0 to 295.3 Ω after 30 cycles, while the values of ΔR_{sf} are 66.3, 41.2, and 61.2 Ω for YF_3 -coated LMNCO electrodes with 1, 2, and 3 wt.% coating contents, respectively. Therefore, the poor rate capacity and cycling performance of pristine LMNCO can be ascribed the rapid increase of impedance for Li-ion diffusion in the SEI film.

To further investigate the redox reaction occurring during charge and discharge process, the cyclic voltammograms (CV) of the pristine and 2wt.% YF_3 -coated $\text{Li}_{1.2}\text{Mn}_{0.54}\text{Ni}_{0.13}\text{Co}_{0.13}\text{O}_2$ electrodes have been measured in Fig. 9. The anodic and cathodic peaks presented in the CV curves are related to the phase transitions of electrode, simultaneously with the processes of Li^+ intercalation and deintercalation. Both CV curves demonstrate two anodic peaks located at 4.2 and 4.55 V during the initial cycle, corresponding to the oxidation of Ni^{2+} and Co^{3+} and the irreversible extraction of Li^+ from Li_2MnO_3 phase, respectively. It can be seen that the peaks located at 4.55 V are missing in the 2nd and 3rd cycles due to the irreversible electrochemical reaction of Li_2MnO_3 component [33]. The cathodic peak located at 3.8 V observed in the discharge profile is related to the

Fig. 9 Cyclic voltammograms of pristine $\text{Li}_{1.2}\text{Mn}_{0.54}\text{Ni}_{0.13}\text{Co}_{0.13}\text{O}_2$ (a), 2 wt.% YF_3 -coated $\text{Li}_{1.2}\text{Mn}_{0.54}\text{Ni}_{0.13}\text{Co}_{0.13}\text{O}_2$ (b)



reduction reaction of Ni^{4+} to Ni^{2+} followed by Co^{4+} to Co^{3+} . Besides, the cathodic peak located at 3.3 V presented in the 2nd and 3rd cycles corresponds to the reduction of Mn^{4+} to Mn^{3+} in the layered MnO_2 component and the transformation of cathode from layer structure to spinel structure [34]. A gentle cathodic peak located at 3.3 V for 2wt.% YF_3 -coated LMNCO electrode is observed, while the pristine LMNCO shows a keen-edged peak at 3.3 V, meaning that the thin YF_3 film could restrain the structure transformation of cathode during the charge and discharge process. Furthermore, the 2wt.% YF_3 -coated LMNCO demonstrates more overlapping CV curves than that of pristine one. It implies that YF_3 coating layer promotes the reversibility of the electrochemical redox for cathode [35].

To sum up, the YF_3 coating layer has a great influence on the electrochemical properties of cathode material, including initial Coulombic efficiency, high-rate capability, and cycling performance. However, the YF_3 coating content on the surface of pristine sample should be optimized.

Conclusions

The layered lithium-rich materials $\text{Li}_{1.2}\text{Mn}_{0.54}\text{Ni}_{0.13}\text{Co}_{0.13}\text{O}_2$ are synthesized via using the carbonate co-precipitation method. Subsequently, the YF_3 layer with different coating contents is used to modify the surface of the pristine $\text{Li}_{1.2}\text{Mn}_{0.54}\text{Ni}_{0.13}\text{Co}_{0.13}\text{O}_2$ sample. TEM and EDS show that the surface of 2wt.% YF_3 -coated LMNCO is successfully covered by the thin YF_3 layer with the thickness of 10–30 nm. Compared with the pristine LMNCO, the YF_3 -coated LMNCO samples deliver the improved electrochemical properties. Within the amount of 0–3 wt.%, the 2 wt.% YF_3 -coated LMNCO demonstrates the optimized cycle stability and high-rate capability due to the lowest impedance of Li^+ migration at the electrode/electrolyte interface. The 2wt.% YF_3 -coated LMNCO delivers a discharge capacity of 116.6 mAh g^{-1} at 5 C rate, much larger than that (95.6 mAh g^{-1}) of the pristine one. And after 100 cycles, the high capacity retention of 92.2% is obtained for the 2wt.% YF_3 -coated LMNCO, while the pristine LMNCO only possesses 84.8%. Therefore, surface modification with YF_3 is an effective method to solve the drawbacks of layered lithium-rich materials for the practical application.

Acknowledgments This work has been supported by the National Natural Science Foundation of China (No.51671152), and Shaanxi Province Industrial Research Project (2016GY-020).

References

1. Etacheri V, Marom R, Elazari R, Salitra G, Aurbach D (2011) Challenges in the development of advanced Li-ion batteries: a review. *Energy Environ Sci* 4:3243–3262
2. Yang JG, Cheng FY, Zhang XL, Gao HY, Tao ZL, Chen J (2014) Porous $0.2\text{Li}_2\text{MnO}_3 \cdot 0.8\text{LiNi}_{0.5}\text{Mn}_{0.5}\text{O}_2$ nanorods as cathode materials for lithium-ion batteries. *J Mater Chem A* 2:1636–1640
3. Tang W, Liu LL, Tian S, Li L, Yue YB, Wu YP, Guan SY, Zhu K (2010) Nano- LiCoO_2 as cathodematerial of large capacity and high rate capability for aqueous rechargeable lithium batteries. *Electrochem Commun* 12:1524–1526
4. Liu YY, Cao CB, Li J (2010) Enhanced electrochemical performance of carbon nanospheres- LiFePO_4 composite by PEG based sol-gel synthesis. *Electrochim Acta* 55:3921–3926
5. Wu F, Tian J, Su YF, Guan YB, Jin Y, Wang Z, He T, Bao LY, Chen S (2014) Lithium-active molybdenum trioxide coated $\text{LiNi}_{0.5}\text{Co}_{0.2}\text{Mn}_{0.3}\text{O}_2$ cathode material with enhanced electrochemical properties for lithium-ion batteries. *J Power Sources* 269:747–754
6. He F, Wang XQ, Du CQ, Baker AP, Wu JW, Zhang XH (2015) The effect of samaria doped ceria coating on the performance of $\text{Li}_{1.2}\text{Ni}_{0.13}\text{Co}_{0.13}\text{Mn}_{0.54}\text{O}_2$ cathode material for lithium-ion battery. *Electrochim Acta* 153:484–491
7. Jiang X, Wang ZH, Rooney D, Zhang XX, Feng J, Qiao JS, Sun W, Sun KN (2015) A design strategy of large grain lithium-rich layered oxides for lithium-ion batteries cathode. *Electrochim Acta* 160:131–138
8. Gu M, Belharouak I, Zheng J, Wu H, Xiao J, Genc A, Amine K, Thevuthasan S, Baer DR, Zhang J-G, Browning ND, Liu J, Wang C (2013) Formation of the spinel phase in the layered composite cathode used in Li-Ion batteries. *ACS Nano* 7:760–767
9. Du CQ, Zhang F, Ma CX, Wu JW, Tang ZY, Zhang XH, Qu DY (2016) Synthesis and electrochemical properties of $\text{Li}_{1.2}\text{Mn}_{0.54}\text{Ni}_{0.13}\text{Co}_{0.13}\text{O}_2$ cathode material for lithium-ion battery. *Ionics* 22:209–218
10. Han ES, Li YP, Zhu LZ, Zhao L (2014) The effect of MgO coating on $\text{Li}_{1.17}\text{Mn}_{0.48}\text{Ni}_{0.23}\text{Co}_{0.12}\text{O}_2$ cathode material for lithium ion batteries. *Solid State Ionics* 255:113–119
11. Shi SJ, Tu JP, Zhang YJ, Zhang YD, Zhao XY, Wang XL, Gu CD (2013) Effect of Sm_2O_3 modification on $\text{Li}[\text{Li}_{0.2}\text{Mn}_{0.56}\text{Ni}_{0.16}\text{Co}_{0.08}]\text{O}_2$ cathode material for lithium ion batteries. *Electrochim Acta* 108:441–448
12. Lee SH, Koo BK, Kim JC, Kim KM (2008) Effect of $\text{Co}_3(\text{PO}_4)_2$ coating on $\text{Li}[\text{Co}_{0.1}\text{Ni}_{0.15}\text{Li}_{0.2}\text{Mn}_{0.55}]\text{O}_2$ cathode material for lithium rechargeable batteries. *J Power Sources* 184:276–283
13. Wang ZY, Liu EZ, He CN, Shi CS, Li JJ, Zhao NQ (2013) Effect of amorphous FePO_4 coating on structure and electrochemical performance of $\text{Li}_{1.2}\text{Ni}_{0.13}\text{Co}_{0.13}\text{Mn}_{0.54}\text{O}_2$ as cathode material for Li-ion batteries. *J Power Sources* 236:25–32
14. Liu XY, Liu JL, Huang T, Yu AS (2013) CaF_2 -coated $\text{Li}_{1.2}\text{Mn}_{0.54}\text{Ni}_{0.13}\text{Co}_{0.13}\text{O}_2$ as cathode materials for Li-ion batteries. *Electrochim Acta* 109:52–58
15. Lu C, Wu H, Zhang Y, Liu H, Chen BJ, Wang S (2014) Cerium fluoride coated layered oxide $\text{Li}_{1.2}\text{Mn}_{0.54}\text{Ni}_{0.13}\text{Co}_{0.13}\text{O}_2$ as cathode materials with improved electrochemical performance for lithium ion batteries. *J Power Sources* 267:682–691
16. Li GR, Feng X, Ding Y, Ye SH, Gao XP (2012) AlF_3 -coated $\text{Li}(\text{Li}_{0.17}\text{Ni}_{0.25}\text{Mn}_{0.58})\text{O}_2$ as cathode material for Li-ion batteries. *Electrochim Acta* 78:308–315
17. Li N, An R, Su YF, Wu F, Bao LY, Chen L, Zheng Y, Shou HF, Chen S (2013) The role of yttrium content in improving electrochemical performance of layered lithium-rich cathode materials for Li-ion batteries. *J Mater Chem A* 1:9760–9767

18. Kang SF, Qin HF, Fang Y, Li X, Wang YG (2014) Preparation and electrochemical performance of Yttrium doped $\text{Li}[\text{Li}_{0.20}\text{Mn}_{0.534}\text{Ni}_{0.133}\text{Co}_{0.133}]\text{O}_2$ as cathode material for lithium ion batteries. *Electrochim Acta* 144:22–30
19. Jin X, Xu QJ, Liu XN, Yuan XL, Liu HM (2016) Improvement in rate capability of lithium-rich cathode material $\text{Li}[\text{Li}_{0.2}\text{Ni}_{0.13}\text{Co}_{0.13}\text{Mn}_{0.54}]\text{O}_2$ by Mo substitution. *Ionics* 22: 1369–1376
20. Ghanty C, Basu RN, Majumder SB (2014) Electrochemical performances of $0.9\text{Li}_2\text{MnO}_3-0.1\text{Li}(\text{Mn}_{0.375}\text{Ni}_{0.375}\text{Co}_{0.25})\text{O}_2$ cathodes: role of the cycling induced layered to spinel phase transformation. *Solid State Ionics* 256:19–28
21. Chen M, Chen DR, Liao YH, Huang QM, Li WS (2015) Influence of Fe substitution on cycling stability of $\text{Li}[\text{Li}_{0.2}\text{Ni}_{0.13}\text{Mn}_{0.54}\text{Co}_{0.13}]\text{O}_2$ cathode for lithium ion batteries. *Ionics* 21:1827–1833
22. Karino W (2016) Order of the transition metal layer in $\text{LiNi}_{1/3}\text{Co}_{1/3}\text{Mn}_{1/3}\text{O}_2$ and stability of the crystal structure. *Ionics* 22:991–995
23. Wu Y, Vadivel Murugan A, Manthiram A (2008) Surface modification of high capacity layered $\text{Li}[\text{Li}_{0.2}\text{Mn}_{0.54}\text{Ni}_{0.13}\text{Co}_{0.13}]\text{O}_2$ cathodes by AlPO_4 . *J Electrochem Soc* 155:A635–A641
24. Zhang H, Qiao QQ, Li GR, Gao XP (2014) PO_4^{3-} polyanion-doping for stabilizing Li-rich layered oxides as cathode materials for advanced lithium-ion batteries. *J Mater Chem A* 2:7454–7460
25. Jin X, Xu QJ, Liu HM, Yuan XL, Xia YY (2014) Excellent rate capability of Mg doped $\text{Li}[\text{Li}_{0.2}\text{Ni}_{0.13}\text{Co}_{0.13}\text{Mn}_{0.54}]\text{O}_2$ cathode material for lithium-ion battery. *Electrochim Acta* 136:19–26
26. Cong LN, Gao XG, Ma SC, Guo X, Zeng YP, Tai LH, Wang RS, Xie HM, Sun LQ (2014) Enhancement of electrochemical performance of $\text{Li}[\text{Li}_{0.2}\text{Mn}_{0.54}\text{Ni}_{0.13}\text{Co}_{0.13}]\text{O}_2$ by surface modification with $\text{Li}_4\text{Ti}_5\text{O}_{12}$. *Electrochim Acta* 115:399–406
27. Yabuuchi N, Yoshii K, Myung ST, Nakai I, Komaba S (2011) Detailed Studies of a high-capacity electrode material for rechargeable batteries, $\text{Li}_2\text{MnO}_3-\text{LiCo}_{1/3}\text{Ni}_{1/3}\text{Mn}_{1/3}\text{O}_2$. *J Am Chem Soc* 133:4404–4419
28. Liu XY, Liu JL, Huang T, Yu AS (2013) CaF_2 -coated $\text{Li}_{1.2}\text{Mn}_{0.54}\text{Ni}_{0.13}\text{Co}_{0.13}\text{O}_2$ as cathode materials for Li-ion batteries. *Electrochim Acta* 109:52–58
29. Nadimicherla R, Chen W, Guo X (2015) Synthesis and characterization of $\alpha\text{-MoO}_3$ nanobelt composite positive electrode materials for lithium battery application. *Mater Res Bull* 66:140–146
30. Zheng JM, Wu XB, Yang Y (2013) Improved electrochemical performance of $\text{Li}[\text{Li}_{0.2}\text{Mn}_{0.54}\text{Ni}_{0.13}\text{Co}_{0.13}]\text{O}_2$ cathode material by fluorine incorporation. *Electrochim Acta* 105:200–208
31. Liu XH, Kou LQ, Shi T, Liu K, Chen L (2014) Excellent high rate capability and high voltage cycling stability of Y_2O_3 -coated $\text{LiNi}_{0.5}\text{Co}_{0.2}\text{Mn}_{0.3}\text{O}_2$. *J Power Sources* 267:874–880
32. Shi SJ, Tu JP, Mai YJ, Zhang YQ, Gu CD, Wang XL (2012) Effect of carbon coating on electrochemical performance of $\text{Li}_{1.048}\text{Mn}_{0.381}\text{Ni}_{0.286}\text{Co}_{0.286}\text{O}_2$ cathode material for lithium-ion batteries. *Electrochim Acta* 63:112–117
33. Amalraj F, Talianker M, Markovsky B, Sharon D, Burlaka L, Shafir G, Zinigrad E, Haik O, Aurbach D, Lampert J, Dobrick MS, Garsuch A (2013) Studies of Li and Mn-Rich $\text{Li}_x[\text{MnNiCo}]\text{O}_2$ electrodes: electrochemical performance, structure, and the effect of the aluminum fluoride coating batteries and energy storage. *J Electrochem Soc* 160:A324–A337
34. Sun YK, Lee MJ, Yoon CS, Hassoun J, Amine K, Scrosati B (2012) The role of AlF_3 coatings in improving electrochemical cycling of Li-enriched nickel-manganese oxide electrodes for Li-Ion batteries. *Adv Mater* 24:1192–1196
35. Yu RB, Lin YB, Huang ZG (2015) Investigation on the enhanced electrochemical performances of $\text{Li}_{1.2}\text{Ni}_{0.13}\text{Co}_{0.13}\text{Mn}_{0.54}\text{O}_2$ by surface modification with ZnO . *Electrochim Acta* 173:515–522